Inorg. Chem. **2007**, *46*, 8698–8704

A Series of New Copper Iodobismuthates: Structural Relationships, Optical Band Gaps Affected by Dimensionality, and Distinct Thermal Stabilities

Wen-Xiang Chai,[†,‡] Li-Ming Wu,[†] Jun-Qian Li,[§] and Ling Chen*[,†]

State Key Laboratory of Structural Chemistry, Fujian Institute of Research on the Structure of Matter, Chinese Academy of Sciences, Fuzhou, Fujian 350002, People's Republic of China, Graduate School of the Chinese Academy of Sciences, Beijing 100039, People's Republic of China, and Department of Chemistry, Fuzhou University, Fuzhou, Fujian 350002, People's Republic of China

Received May 9, 2007

Three new copper iodobismuthates, red tetranuclear $[n\text{-}Bu_4N][Cu_2(CH_3CN)_2Bi_2I_{10}]$ (**1**), dark-red infinite linear $[Et_4N]_{2n}[Cu_2Bi_2I_{10}]_n$ (**2**), and black polymeric ladderlike $[Cu(CH_3CN)_4]_{2n}[Cu_2Bi_2I_{10}]_n$ (**3**), crystallize from solutions of BiI_3 and CuI in the presence of different cations. A regular structural relationship from 0-D (**1**) to 1-D linear anion chains (**2**) to 1-D ladderlike anion chains (**3**) is observed. The self-assembly of the basic building unit $Cu_2Bi_2I_{10}$ as altered by different cations is proposed to be the driving force for their formation. The optical band gaps exhibit a structure-related decrease from **1** to **2**/**3**, in agreement with their color changes and the density functional theory (DFT) calculation results. The electronic structures and the relationship with corresponding monobismuth analogues and the Ag–Bi isotypes are discussed on the basis of DFT calculations. In spite of their structural similarities, the compounds are distinctive thermally: **2** is stable to 230 °C, **1** undergoes a solvent loss at 85 °C to form a new phase that is thermally stable to 230 °C, and **3** releases a solvent molecule and decomposes at 80 °C into BiI_3 and CuI. The essential reasons for these differences are discussed.

Introduction

The chemistries of the heavy p-block element iodometalates AM_xI_y (A = cation; M = Sn, Pb, Sb, or Bi) have been widely investigated for several decades and have been found to exhibit numerous remarkable optical and electronic properties such as semiconductivity (even metallic conductivity), luminescence, nonlinear optical activity, and ferroelectricity.[1−33] The major structural characteristic of this family is the diverse anionic structure motifs, which range from discrete mono- or polynuclear species to infinite higher dimensional (1-, 2-, or 3-D) varieties, which are altered by changing the reaction conditions and, especially, the size/charge of the cations. Several recent efforts have shown that the heterometallic bonding interactions, M−I (M = Pb or Bi) together with TM−I (TM = Ag or Cu), yield unprecedented bimetallic complexes and lead to their novel optical properties.[10−13,33] Compared with the monometallic M−I compounds (M = Pb or Bi), the geometry or connectivities

* To whom correspondence should be addressed. E-mail: chenl@fjirsm.ac.cn. Tel: (011)86-591-83704947.
† Chinese Academy of Sciences.
‡ Graduate School of the Chinese Academy of Sciences.
§ Fuzhou University.

(1) Mitzi, D. B.; Feild, C. A.; Harrison, W. T. A.; Guloy, A. M. *Nature* **1994**, *369*, 467.
(2) Mitzi, D. B.; Wang, S.; Feild, C. A.; Chess, C. A.; Guloy, A. M. *Science* **1995**, *267*, 1473.
(3) Mitzi, D. B. *Prog. Inorg. Chem.* **1999**, *48*, 1.
(4) Kagan, C. R.; Mitzi, D. B.; Dimitrakopoulos, C. D. *Science* **1999**, *286*, 945.
(5) Guloy, A. M.; Tang, Z. J.; Miranda, P. B.; Srdanov, V. I. *Adv. Mater.* **2001**, *13*, 833.
(6) Mercier, N.; Barres, A. L.; Giffard, M.; Rau, I.; Kajzar, F.; Sahraoui, B. *Angew. Chem., Int. Ed.* **2006**, *45*, 2100.
(7) Fisher, G. A.; Norman, N. C. *Adv. Inorg. Chem.* **1994**, *41*, 233.
(8) Eickmeier, H.; Jaschinski, B.; Hepp, A.; Nuss, J.; Reuter, H.; Blachnik, R. *Z. Naturforsch.* **1999**, *54b*, 305.
(9) Wojtas, M.; Jakubas, R.; Ciunik, Z.; Medycki, W. *J. Solid State Chem.* **2004**, *177*, 1575.
(10) Fan, L. Q.; Wu, L. M.; Chen, L. *Inorg. Chem.* **2006**, *45*, 3149.
(11) Fan, L. Q.; Huang, Y. Z.; Wu, L. M.; Chen, L.; Li, J. Q.; Ma, E. *J. Solid State Chem.* **2006**, *179*, 2361.
(12) Goforth, A. M.; Gardinier, J. R.; Smith, M. D.; Peterson, L.; zur Loye, H. C. *Inorg. Chem. Commun.* **2005**, *8*, 684.
(13) Feldmann, C. *Inorg. Chem.* **2001**, *40*, 818.
(14) Papavassiliou, G. C.; Koutselas, I. B.; Terzis, A.; Raptopoulou, C. P. *Z. Naturforsch.* **1995**, *50b*, 1566.
(15) Krautscheid, H. *Z. Anorg. Allg. Chem.* **1999**, *625*, 192.

10.1021/ic700904d CCC: $37.00
Published on Web 09/11/2007

Table 1. Crystallographic Data and Refinement Details for Compounds **1**−**3**

empirical formula	$C_{18}H_{39}CuBiI_5N_2$ (**1**)	$C_8H_{20}CuBiI_5N$ (**2**)	$C_8H_{12}Cu_2BiI_5N_4$ (**3**)
fw	1190.54	1037.28	1134.80
cryst syst	triclinic	triclinic	triclinic
Z	2	2	2
space group	$P\bar{1}$ (No. 2)	$P\bar{1}$ (No. 2)	$P\bar{1}$ (No. 2)
a (Å)	12.035(5)	8.518(1)	8.340(4)
b (Å)	12.357(5)	10.871(1)	11.000(6)
c (Å)	13.231(5)	11.425(1)	13.342(7)
α (deg)	109.667(4)	93.642(3)	111.406(5)
β (deg)	91.205(1)	99.261(6)	90.506(6)
γ (deg)	117.254(2)	98.105(6)	90.458(5)
V (Å^3)	1610.7(1)	1029.8(2)	1139.4(10)
D_c (g cm^{-3})	2.455	3.345	3.308
μ (mm^{-1})	10.915	17.044	16.322
R1, wR2 [$I > 2\sigma(I)$][a]	0.0378, 0.0948	0.0396, 0.0991	0.0504, 0.1335
diff peak, hole (e Å^{-3})	+0.938, −2.226	+2.768 (0.90 Å from Bi1), −4.274 (0.84 Å from Bi1)	+2.148 (1.02 Å from Bi1), −2.458 (0.94 Å from Bi1)

[a] $R1 = \sum||F_o| - |F_c||/\sum|F_o|$. $wR2 = [\sum w(F_o^2 - F_c^2)^2/\sum w(F_o^2)^2]^{1/2}$.

of the building blocks, e.g., MI_6 octahedral units, are significantly changed by the TM−I bonding. Moreover, the TM atoms also contribute to the electronic structures and therefore introduce novel properties of the compounds. For example, the infinite linear $[PbI_6]_n$ chain may be decorated by either tetrahedral AgI_4 or trigonal CuI_3 species to give either a novel fatter heterometallic chain or a rigid chain.[10] Recent studies of Pb/TM/I systems reveal that the unusual "octahedral PbI_4" with a cis divacant coordination sphere[11] may be generated by involvement of the TM−I bonding, leading to a new red−infrared (IR) fluorescence. Although Bi is a neighboring element of Pb with similar cationic size and octahedral coordination character,[7] their oxidation states are different, and different but related chemistries might be expected. To date, ∼60 iodobismuthates overall are known structurally with a large spectrum of organic cations, and these show about 20 different monometallic structural types. Their anionic moieties range from isolated clusters (e.g., $[BiI_6]^{3-}$, $[Bi_2I_{10}]^{4-}$, $[Bi_4I_{16}]^{4-}$, $[Bi_6I_{22}]^{4-}$, etc.)[14−26] to infinite chains (e.g., $[BiI_4^-]_n$, $[BiI_5^{2-}]_n$, $[Bi_4I_{14}^{2-}]_n$, $[Bi_6I_{22}^{4-}]_n$, etc.),[25,27−30] and to 2-D layers (e.g., $[BiI_4^-]_n$ and $[Bi_2I_9^{3-}]_n$).[31,32] However, only three heterometallic examples are known: $[CuBi_5I_{19}^{3-}]_n$,[13] $[Ag_2Bi_4I_{16}^{2-}]_n$, and $[Ag_2Bi_2I_{10}^{2-}]_n$.[33] Here we utilize a series of 1+ cations, n-Bu_4N^+, Et_4N^+, and $Cu(CH_3CN)_4^+$, with more-or-less gradual decreases in size but increases in flexibility to generate three new heterometallic Bi/Cu/I structures. Their single-crystal structures, optical band gaps, and electronic structures on the basis of density functional theory (DFT) calculations are reported. The systematic structural relationships, band-gap changes, and thermal stabilities among these are also discussed.

Experimental Details

Materials and Methods. All chemicals and solvents were used without further purification. The powder X-ray diffraction (XRD) data were collected by means of a BDX 3300 X-ray diffractometer (Cu Kα_1, λ = 1.54056 Å) at a scanning rate of 2°/min. The elemental analyses were carried out on a Vario EL III element analyzer, and the IR spectra were recorded on a Perkin-Elmer FT-IR spectrophotometer. The thermogravimetric analyses (TGA) and differential scanning calorimetry (DSC) measurements were performed on pure polycrystalline samples with a STA449C Instrument by Netzsch under flowing N_2 with a heating rate of 15 °C/min over a temperature range of 30−800 °C. The diffuse-reflectance UV−visible spectroscopy (190−1100 nm) was performed at room temperature in a reflectance mode on a Perkin-Elmer Lambda 35 UV−visible spectrometer equipped with an integrating sphere and with $BaSO_4$ as the reference material.

Preparation of $[n$-$Bu_4N]_2[Cu_2(CH_3CN)_2Bi_2I_{10}]$ (1). A mixture of BiI_3 (0.1 mmol, 60 mg), CuI (0.1 mmol, 19 mg), and n-Bu_4NI (0.1 mmol, 37 mg) was stirred in a 10 mL mixed solvent of Me_2CO and CH_3CN (1:1, v/v) in air for 30 min, and then about 20 mL of i-PrOH was added into the resulting solution. After 3 days, 78 mg of red block-shaped crystals was obtained at 4 °C (a 65.5% yield on the basis of BiI_3). Anal. Calcd for **1** (dried): C, 18.16; H, 3.30; N, 2.35. Found: C, 17.95; H, 3.25; N, 2.34. IR (KBr, cm^{-1}): 2958s, 2929s, 2871s, 2347w, 1467s, 1439m, 1379m, 1167w, 1032w, 894w, 877w, 435m. The IR spectrum and the assignment of characteristic vibrations are shown in Figure S4-1 of the Supporting Information.

Preparation of $[Et_4N]_{2n}[Cu_2Bi_2I_{10}]_n$ (2). Similarly but with a different cation, BiI_3 (0.1 mmol, 60 mg), CuI (0.1 mmol, 19 mg), and Et_4NI (0.1 mmol, 26 mg) were dissolved in a 10 mL Me_2CO/CH_3CN mixture (1:1, v/v) over 30 min in air, and then about 15

(16) Lazarini, F. *Acta Crystallogr., Sect. C: Cryst. Struct. Commun.* **1980**, *9*, 815.
(17) Zhu, X. H.; Mercier, N.; Frere, P.; Blanchard, P.; Roncali, J.; Allain, M.; Pasquier, C.; Riou, A. *Inorg. Chem.* **2003**, *42*, 5330.
(18) Bowmaker, G. A.; Junk, P. C.; Lee, A. M.; Skelton, B. W.; White, A. H. *Aust. J. Chem.* **1998**, *51*, 293.
(19) Geiser, U.; Wade, E.; Wang, H. H.; Williams, J. M. *Acta Crystallogr., Sect. C: Cryst. Struct. Commun.* **1990**, *46*, 1547.
(20) Okrut, A.; Feldmann, C. *Z. Anorg. Allg. Chem.* **2006**, *632*, 409.
(21) Kubiak, R.; Ejsmont, K. *J. Mol. Struct.* **1999**, *474*, 275.
(22) Krautscheid, H. *Z. Anorg. Allg. Chem.* **1994**, *620*, 1559.
(23) Pohl, S.; Peters, M.; Haase, D.; Saak, W. *Z. Naturforsch.* **1994**, *49b*, 741.
(24) Clegg, W.; Errington, R. J.; Fisher, G. A.; Green, M. E.; Hockless, D. C. R.; Norman, N. C. *Chem. Ber.* **1991**, *124*, 2457.
(25) Krautscheid, H. *Z. Anorg. Allg. Chem.* **1995**, *621*, 2049.
(26) Feldmann, C. *J. Solid State Chem.* **2003**, *172*, 53.
(27) Geiser, U.; Wang, H. H.; Budz, S. M.; Lowry, M. J.; Williams, J. M.; Ren, J. Q.; Whangbo, M. H. *Inorg. Chem.* **1990**, *29*, 1611.
(28) Rogers, R. D.; Bond, A. H.; Aguinaga, S.; Reyes, A. *J. Am. Chem. Soc.* **1992**, *114* (8), 2967.
(29) Mitzi, D. B.; Brock, P. *Inorg. Chem.* **2001**, *40*, 2096.
(30) Goforth, A. M.; Peterson, L.; Smith, M. D.; zur Loye, H. C. *J. Solid State Chem.* **2005**, *178*, 3529.
(31) Mitzi, D. B. *Inorg. Chem.* **2000**, *39*, 6107.
(32) Sidey, V. I.; Voroshilov, Y. V.; Kun, S. V.; Peresh, E. Y. *J. Alloys Compd.* **2000**, *296*, 53.
(33) Chai, W.-X.; Wu, L.-M.; Li, J.-Q.; Chen, L. *Inorg. Chem.* **2007**, *46*, 1042.

Scheme 1. Schematic Diagram of the Rational Design Strategy and the Outline of the Synthetic Routes of Compounds **1**−**3**

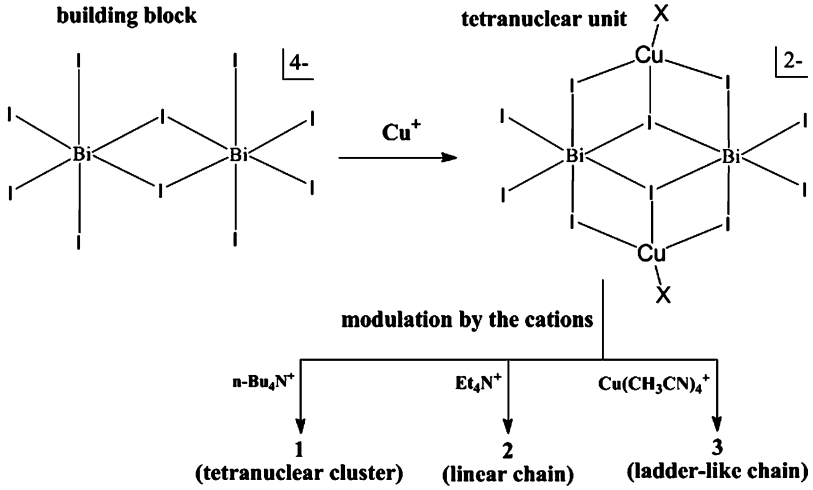

mL of *i*-PrOH was added to the solution. A total of 68 mg of dark-red block-shaped crystals was obtained after 3 days at 4 °C (a 65.6% yield on the basis of BiI_3). Anal. Calcd for **2** (dried): C, 9.26; H, 1.94; N, 1.35. Found: C, 9.42; H, 1.90; N, 1.34. IR (KBr, cm^{-1}): 2999m, 2977s, 2940m, 1452s, 1395s, 1367m, 1302m, 1179s, 1116w, 1074w, 1027m, 999m, 789s. The IR spectrum and the assignment of characteristic vibrations are shown in Figure S4-3 of the Supporting Information.

Preparation of $[Cu(CH_3CN)_4]_{2n}[Cu_2Bi_2I_{10}]_n$ (3). A mixture of BiI_3 (0.1 mmol, 60 mg) and CuI (0.2 mmol, 38 mg) was stirred in a 10 mL mixed solvent of Me_2CO and CH_3CN (1:1, v/v) for 30 min in air. A mass of 69 mg of black block-shaped crystals was obtained 3 days after covering the resulting solution with a layer of *i*-PrOH (a 60.8% yield on the basis of BiI_3). Anal. Calcd for **3** (dried): C, 8.47; H, 1.07; N, 4.94. Found: C, 8.21; H, 1.13; N, 4.15. IR (KBr, cm^{-1}): 3577s, 2986w, 2924w, 2291w, 2254m, 1606s, 1432m, 1404m, 1365m. The IR spectrum and the assignment of characteristic vibrations are shown in Figure S4-4 of the Supporting Information.

The three products dissolve well in *N*,*N*-dimethylformamide (DMF), CH_3CN, or Me_2CO but not in EtOH or H_2O.

Crystal Structure Determinations of Compounds 1−3. Suitable single crystals of **1**−**3** were selected and mounted on thin glass fibers with the aid of an epoxy resin. The XRD data were collected at 293(2) K on a Rigaku Mercury CCD diffractometer (Mo Kα, $\lambda = 0.71073$ Å). An empirical absorption correction based on multiple measurements of equivalent reflections was applied to each data set by the *CrystalClear* program.[34] The structures were solved by direct methods and refined on F^2 by full-matrix least squares using the *SHELXL-97* software package without any unusual events.[35] All H atoms were refined with a riding mode. Some crystal data and refinement details are gathered in Table 1. The fractional atomic coordinates and thermal parameters are listed in Tables S1, S3, and S5 of the Supporting Information, and selected bond lengths and angles are listed in Tables S2, S4, and S6 of the Supporting Information.

Computation Descriptions. The crystallographic data of **1**−**3** were employed for theoretical calculation with further optimization. All density of states (DOS) calculations were performed using the *DMOL3* code[36] according to DFT,[37] including relativistic approximations on core electrons.[38] The exchange-correlation energies were calculated using the Perdew−Wang generalized-gradient approximation.[39] The smearing width for the DOS is 0.002 ha. The other calculation parameters and convergence criteria were set by the default values of the *DMOL3* code.

Results and Discussion

Rational Syntheses and Structural Modification. As is generally accepted in crystal design, the size, charge, and geometry of the countercations have crucial impacts on the anionic structures through charge balance, fragment packing, and spatial arrangement. Thus, a series of compounds constructed from the same/similar anionic fragment would be an ideal system on which to study the rational synthesis; however, finding such a system is a challenge. Previous reports have indicated that the $[Bi_2I_{10}]^{4-}$ anion might be a suitable candidate as an anionic building block because it crystallizes with different 1+ cations without notable geometry changes.[18,40] On the other hand, heterometal atoms are highly desirable in the Bi/I system because the additional bonding interactions are responsible for the diverse novel structures. They also give rise to interesting properties in Pb/TM/I systems, as was shown recently.[10,11] We have started our exploration by formally introducing Cu^+ ions into $Bi_2I_{10}^{4-}$ anions in a CH_3CN solution. As we expected, a tetranuclear cluster in **1**, $[n\text{-}Bu_4N]_2[Cu_2(CH_3CN)_2Bi_2I_{10}]$, without breaking the primary building block, the $[Bi_2I_{10}]^{4-}$ dimer, was obtained, and more interestingly such a tetranuclear heterometallic anion can also serve as a conceptual building unit in two novel bimetallic polymers in **2**, $[Et_4N]_{2n}[Cu_2Bi_2I_{10}]_n$, and **3**, $[Cu(CH_3CN)_4]_{2n}[Cu_2Bi_2I_{10}]_n$ with different cations (see Scheme 1 and details below). These three compounds exhibit nice stepwise modifications of the anionic structures from a discrete tetranuclear cluster (**1**) to a linear polymeric chain (**2**) to a ladderlike polymeric chain (**3**) with a more-or-less gradual decrease of the cation size and an increase in its flexibility. Remarkably, such structural

(34) *CrystalClear*, version 1.3.5; Rigaku Corp.: Woodlands, TX, 1999.
(35) *SHELXTL*, version 5.1; Bruker-AXS: Madison, WI, 1998.
(36) Papageorgiou, N.; Ferro, Y.; Salomon, E.; Allouche, A.; Layet, J. M.; Giovanelli, L.; Le Lay, G. *Phys. Rev. B* **2003**, *68*, 235105.
(37) Kohn, W.; Sham, L. *Phys. Rev. A* **1965**, *140*, 1133.
(38) Koelling, D. D.; Harmon, B. N. *J. Phys. C: Solid State Phys.* **1977**, *10*, 3107.
(39) Perdew, J. P.; Chevary, J. A.; Vosko, S. H.; Jackson, K. A.; Pederson, M. R.; Singh, D. J.; Fiolhais, C. *Phys. Rev. B* **1992**, *46*, 6671.
(40) Charmant, J. P. H.; Norman, N. C.; Starbuck, J. *Acta Crystallogr., Sect. E.: Struct Rep. Online* **2002**, *58*, M144.

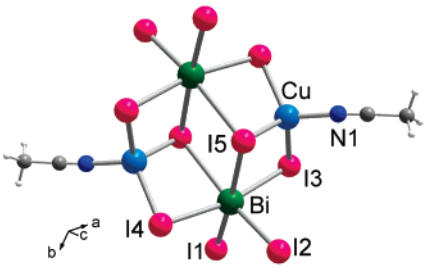

Figure 1. Structure of the isolated anion, $[Cu_2(CH_3CN)_2Bi_2I_{10}]^{2-}$, in **1**. Color code: Bi, green; Cu, blue; I, red; N, deep blue; C, gray; H, white.

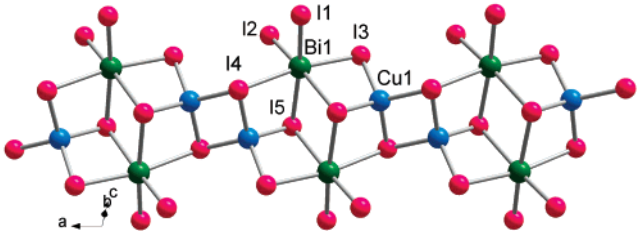

Figure 2. Linear polymeric chain, $[Cu_2Bi_2I_{10}^{2-}]_n$, of **2** along the *a* axis. Color code: Bi, green; Cu, blue; I, red.

evolvement is reflected by the related variations in their intrinsic colors and optical band gaps. Such structural−optical correlations have also been studied on the basis of DFT calculations (below).

Structure Descriptions. The structure of **1** has been characterized (Figure 1) as a new Bi/Cu/I anionic cluster, $[Cu_2(CH_3CN)_2Bi_2I_{10}]^{2-}$, constructed by condensation of a bioctahedron $[Bi_2I_{10}]^{4-}$ and two nominally tetrahedral $[CuI_3N]^{2-}$, both via shared I−I edges. The acetonitrile molecule bonded to each Cu^+ completes the coordination sphere and thereby terminates its coordinating ability. The compound adopts a $P\bar{1}$ space group with an inversion center at the midpoint of the cluster. The crystallographically identical Bi atoms exhibit common BiI_6 octahedra, with Bi−I bond lengths ranging from 2.903(1) to 3.322(1) Å with a 3.10 Å average (Table S2 of the Supporting Information), which is similar to that of a dimeric $Bi_2I_{10}^{4-}$ anion.[18,40] However, the two BiI_6 octahedra in **1** are pushed away from, but bent toward, each other judging from the significantly increased Bi−Bi distance [5.071(2) Å vs 4.777(4) Å in the $Bi_2I_{10}^{4-}$ dimer] and decreased I3−Bi−I4 bond angle [168.56(2)° vs 176.1(2)° in the $Bi_2I_{10}^{4-}$ dimer].[40] The change is in accordance with the I3−Cu−I4 angle. Such a tetra- to binuclear structural change is similar to that between $Bi_4I_{16}^{4-}$ and $Bi_2I_{10}^{4-}$ anions.[12,18,21,40] The rough tetrahedral geometry about Cu is regular, with an average Cu−I bond length of 2.67 Å and a Cu−N1 bond length of 2.001(7) Å. As indicated in Figure S1 of the Supporting Information, the $[Cu_2(CH_3CN)_2Bi_2I_{10}]^{2-}$ anions are surrounded and well-separated by the *n*-Bu_4N^+ cations. The loss of solvent molecules coordinated to Cu on the cluster upon heating leads to decomposition of **1** and a structural change (see the Thermal Properties section).

The anionic structure of **2** (Figure 2) features an infinite 1-D heterometallic chain constructed by the tetranuclear building units $[Cu_2Bi_2I_{10}]^{2-}$ joined at the CuI_4 site via sharing of the I4−I4 edge (*head-to-head* motif) along the *a* direction.

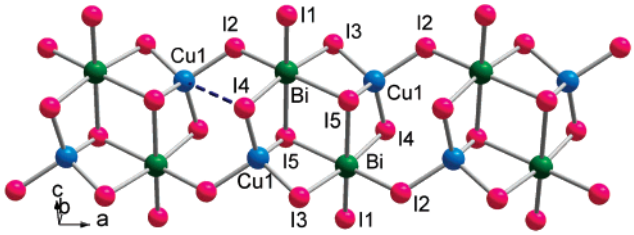

Figure 3. Ladderlike polymeric chain, $[Cu_2Bi_2I_{10}^{2-}]_n$, of **3**.

The repeat unit is structurally similar to the isolated anionic cluster in **1**. The BiI_6 octahedra in **2** are more distorted judging from the larger range of the Bi−I bond lengths, 2.8687(7)−3.3898(7) Å, owing to more sharing of I atoms, with an average of 3.11 Å (Table S4 of the Supporting Information). However, the Bi−Bi distance in **2** is significantly shorter than that in **1** (4.8479(8)vs 5.071(2) Å). Such a shortening is probably favored by the additional condensation and greater sharing of I atoms. The Cu−Cu distance, 3.10(1) Å, is significantly less than that in the discrete $[Cu_2I_6]^{4-}$ dimer, 3.80(3) Å,[41] because of the constraints of condensation. The CuI_4 tetrahedron is normal, with Cu−I bond lengths that vary only slightly, 2.636(2)−2.664(1) Å, with a 2.65 Å average. The heterometallic chains in **2** are arranged into a pseudolayered motif (Figure S2 of the Supporting Information) with the Et_4N^+ cations between them. This structure is the most thermally stable among **1**−**3** (see the Thermal Properties section).

The anion of **3** is also constructed by the tetranuclear $[Cu_2Bi_2I_{10}]^{2-}$ building units but in a different way, namely, a *shoulder-to-shoulder* motif, in which the repeat units are connected at both CuI_4 and BiI_6 sites via common I2 atoms to generate a ladderlike chain along the *a* axis (Figure 3). A key parameter to illustrate the difference is the Cu−Cu distance between adjacent tetranuclear units, 5.19(2) Å, which is 67% greater than that in **2**. The geometry within the $[Bi_2I_{10}^{4-}]$ bioctahedral subunit shows no significant change from **2**, and the Bi−I bond lengths are in the normal range from 2.923(2) to 3.334(2) Å (3.10 Å average; Table S6 of the Supporting Information). Also, the Bi−Bi distance within the bioctahedron, 4.803(2) Å, is similar to that in **2**, which suggests the different packing pattern does not influence the geometry of the building unit itself. The geometry about tetrahedral $Cu1I_4$ is normal, and the distance between Cu and a fifth I (I4) in a neighboring unit (shown as a dashed line in Figure 3) is 3.786(2) Å, far beyond a reasonable bonding range.

The cationic Cu atoms in **3** are coordinated by four solvent molecules as $[Cu(CH_3CN)_4]^+$ and are well distributed around the anionic chains in the crystal, as shown in Figure S3 of the Supporting Information. Under heating, such cations lose CH_3CN, leading to a dramatic loss of stability for **3** (see the Thermal Properties section).

In summary, in comparison with the discrete cluster in **1**, phases **2** and **3** exhibit obvious decreases (about 30%) in the crystal *a* parameters, that is, in the extended direction of

(41) Hartl, H.; Brudgarn, I.; Mahdjour-Hassan-Abadi, F. *Z. Naturforsch.* **1985**, *40b*, 1032.

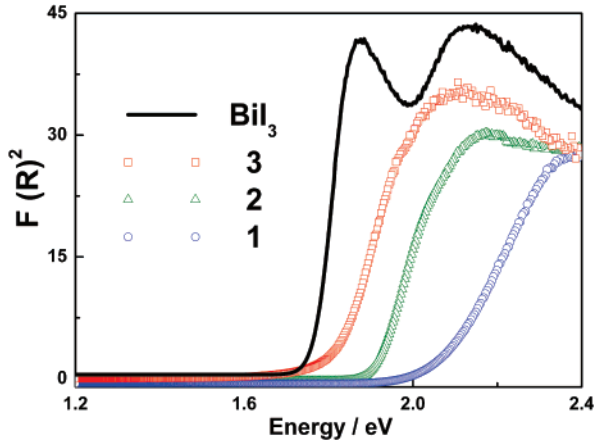

Figure 4. Plot of $F(R)^2$ vs photon energy for **1**−**3** and BiI_3.

each anionic chain. This variation may originate with the size difference of the cations. The larger *n*-Bu_4N^+ cations in **1** sufficiently separate the contacts between the isolated anionic cluster units, but the smaller cations in **2**/**3** allow condensed chains.

Optical Properties. The diffuse-reflectance spectra of **1**−**3** and of BiI_3 have been measured and plotted in Figure 4 as a $F(R)^2$ vs photon energy diagram according to the Kubelka−Munk funtion.[42−44] Their optical band gaps (E_g) determined by the extrapolation method[45,46] are 2.06, 1.89, 1.80, and 1.73 eV, respectively, with the result for BiI_3, 1.73 eV, being consistent with the reported value.[12]

The clear decrease of E_g from **1** to **3** is consistent with their darkening from red (**1**) to black (**3**). Such changes should mainly relate to the structural differences of the anionic moieties because the energetically lower-lying cation bands will only have minor effects on the band structures around the Fermi levels. The E_g values of these compounds appear to parallel the intervals of the building units (Table 2).

Plots of the total and partial DOSs for **1**−**3** are presented in Figure 5 (middle). Consistently, the top of the valence band for each compound is generated by I and Cu, and the bottom of the conduction band consists of the partial DOSs of Bi and I. The decreasing trend of the calculated E_g from **1** to **2**/**3** agrees approximately with the experimental observations. The effective transition edges of **1**−**3** can all be assigned as charge transfers from occupied 3d orbitals of Cu and 5p states of I to empty 6p orbitals of Bi and 5p states of I. In the case of **3**, the cationic Cu2 atom does not contribute to the frontier orbitals, as expected.

The silver iodobismuthate $[Et_4N]_{2n}[Ag_2Bi_2I_{10}]_n$ is known to be identical with **2** structurally, with a comparable 1D chain constructed from a $[M_2Bi_2I_{10}]^{2-}$ tetranuclear repeat unit,[33] consistent with their usual coordination similarities.

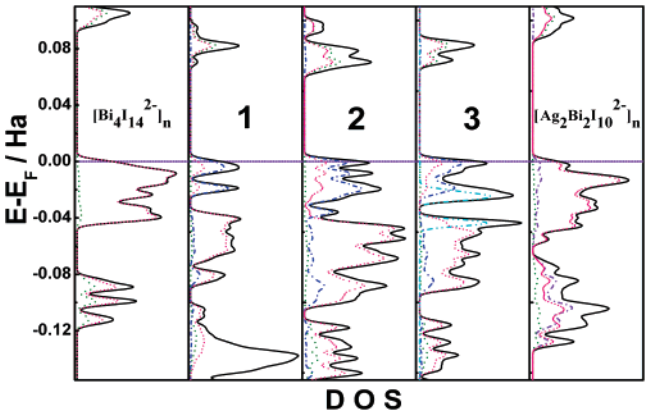

Figure 5. Total and partial DOS plots of (left) $[n\text{-}Bu_4N]_{2n}[Bi_4I_{14}]_n$, (middle) compounds **1**−**3**, and (right) $[Et_4N]_{2n}[Bi_2Ag_2I_{10}]_n$ with the Fermi levels set at zero. Black lines represent the total DOSs, and the colored lines represent the partial DOSs as follows: olivine dashed, Bi; pink dotted, I; blue dash-dotted, Cu; purple dash-dotted, Ag (in the right panel). Additionally, the cyan dash-dot-dotted line in **3** represents the partial DOSs of the solvent-coordinated Cu2 cation.

Table 2. Intervals of the Building Units and the E_g Values of **1**−**3**

	compound		
	1	**2**	**3**
interval of the building units (Å) (*a*)	12.035(5)	8.518(1)	8.340(4)
observed E_g (eV)	2.06	1.89	1.80
calculated E_g (eV)	2.02	1.86	1.90

However, the observed different band gaps (2.05[33] vs 1.86 eV) suggest that Cu and Ag play different roles in the electronic structures. Therefore, DFT calculations were carried out. As shown in Figure 5 (left), the band structure of the monometallic $[n\text{-}Bu_4N]_{2n}[Bi_4I_{14}]_n$,[25] which possesses a chain motif similar to that of **2**, exhibits a distribution of Bi−I bonding states, I nonbonding states (which construct the HOCO, highest occupied crystal orbital), and Bi−I antibonding states (which construct the LUCO, lowest unoccupied crystal orbital) around the Fermi level as the energy increases. With the introduction of Cu, Figure 5 (middle), the corresponding I nonbonding and Bi−I antibonding states show no significant energetic changes, but the Cu−I antibonding states have now been inserted between them. Accordingly, the tops of the valence bands of the Cu analogues now derive nearly entirely from I and Cu orbitals and, consequently, the energy gaps have decreased. Dissimilarly, the results for the Ag/Bi analogue of **2** (Figure 5, right) suggest that the introduction of Ag does not influence the components of the HOCO because the Ag-related states lie at lower energies. Thus, the energy gap is 2.05 eV,[33] 0.03 eV larger than that for $[n\text{-}Bu_4N]_{2n}[Bi_4I_{14}]_n$,[33] an increase that might derive from the distortion of the Bi−I skeleton by the involvement of Ag^+ ions. These opposed E_g changes with respect to the monometallic $[Bi_4I_{14}^{2-}]$ come from the fact that Cu contributes to the top of the valance band, pushes it up, and thus leads to a smaller E_g, but Ag hardly contributes to the HOCO, and its lower energy slightly influences E_g by altering the overall electronic structure.

Thermal Properties. TGA and DSC curves obtained on the polycrystalline samples of **1**−**3** are shown in Figure 6, whereas the purities of samples checked first by XRD measurements are shown in Figures 7b, 8b, and 9b, respec-

(42) Kotūm, G. *Reflectance Spectroscopy*; Springer-Verlag: New York, 1969.
(43) Wendlandt, W. W.; Hencht, H. G. *Reflectance Spectroscopy*; Interscience: New York, 1966.
(44) Tandon, S. P.; Gupta, J. P. *Phys. Status Solidi* **1970**, *38*, 363.
(45) McCarthy, T. J.; Tanzer, T. A.; Kanatzidis, M. G. *J. Am. Chem. Soc.* **1995**, *117*, 1294.
(46) Cao, G.; Rabenberg, L. K.; Nunn, C. M.; Mallouk, T. E. *Chem. Mater.* **1991**, *3*, 149.

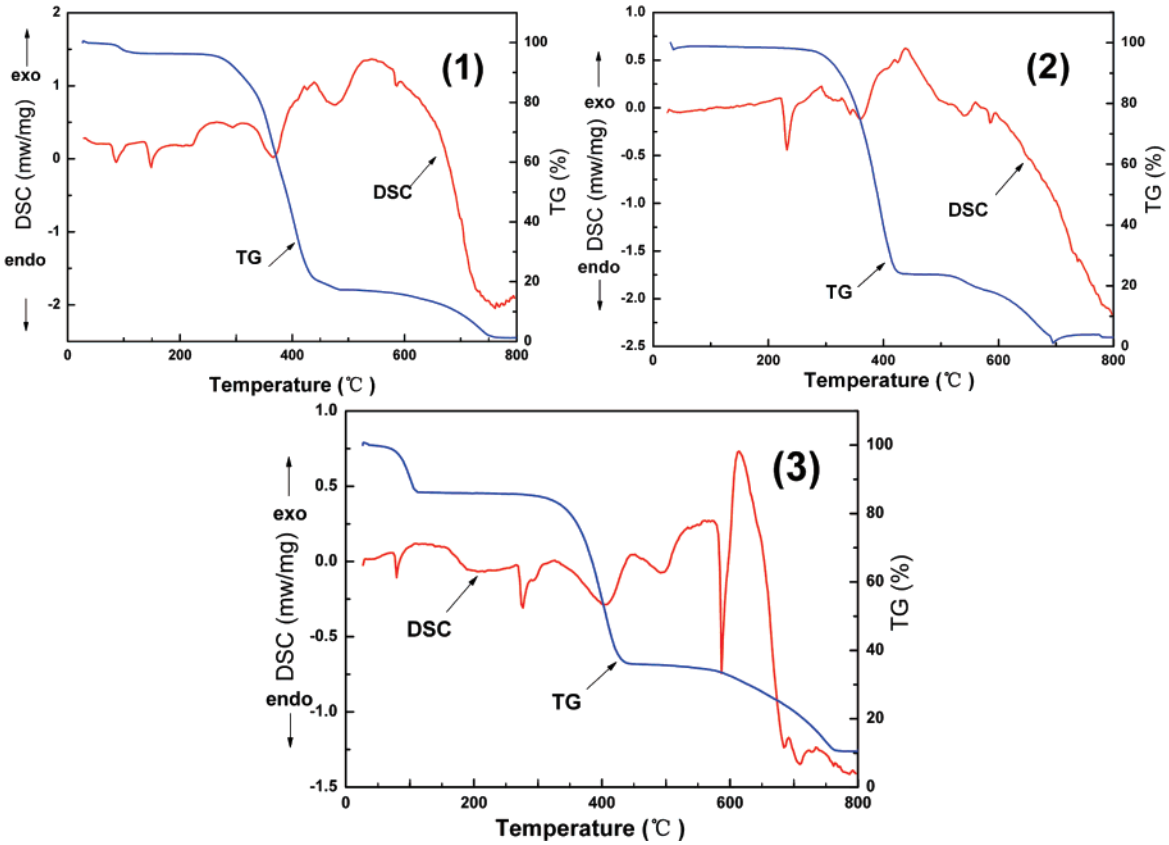

Figure 6. TGA/DSC curves of compounds **1**−**3**.

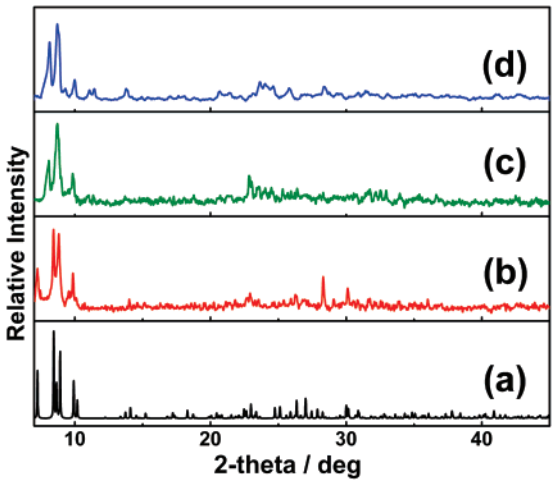

Figure 7. XRD patterns for a polycrystalline sample of **1**: (a) calculated pattern from the single-crystal data; (b) observed at room temperature; (c) annealed at 100 °C under a N_2 atmosphere for 24 h and quenched to room temperature; (d) annealed at 210 °C under a N_2 atmosphere for 24 h and quenched to room temperature.

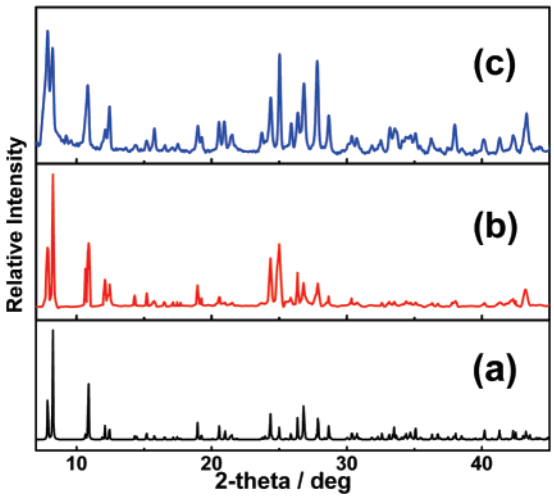

Figure 8. XRD patterns for a polycrystalline sample of **2**: (a) calculated pattern; (b) observed at room temperature; (c) annealed at 210 °C under a N_2 atmosphere for 24 h and quenched to room temperature.

tively. Only **2** shows no weight change up to ∼230 °C. Compound **1** exhibits a weight loss of about 3.67% (calcd: 3.45%) around 85 °C corresponding to the loss of CH_3CN ligands. The XRD pattern taken right after **1** was annealed at 100 °C under a N_2 atmosphere for 24 h and quenched to ambient temperature (Figure 7c) shows a set of totally different diffraction peaks relative to the original at room temperature (Figure 7b). Such an unknown phase was assigned as **1-A**. Melting of **1-A** is observed at about 145 °C, such that **1** annealed at 210 °C under a N_2 atmosphere for 24 h and quenched to room temperature gives an XRD pattern right afterward that matches that of **1-A** well (Figure 7d). Thus, **1-A** appears to be a new Bi/Cu/I structure that exists between 85 and 210 °C, melts congruently at 145 °C, and decomposes above 230 °C. Contrarily, compound **2** is stable up to 230 °C judging from the consistency of the XRD patterns of the room-temperature specimen and the one annealed at 210 °C for 24 h (Figure 8c). The endothermic peak for compound **3** at about 80 °C corresponds to the weight loss of about 14.03% (calcd: 14.47%) of CH_3CN molecules and its decomposition to trigonal BiI_3 plus cubic

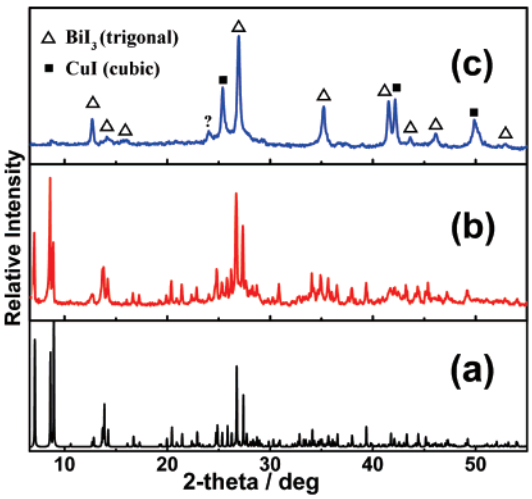

Figure 9. XRD patterns for a polycrystalline sample of **3**: (a) calculated pattern; (b) observed at room temperature; (c) annealed at 100 °C under a N_2 atmosphere for 24 h and quenched to room temperature. Δ indicates trigonal BiI_3 (PDF No. 48-1795), ■ indicates cubic CuI (PDF No. 06-0246), and **?** indicates an unknown phase.

CuI, as is clearly shown in Figure 9. Although **1**−**3** contain the same $[Cu_2Bi_2I_{10}]^{2-}$ building units, the markedly low decomposition temperature of **3** must be caused by the instability of $Cu(CH_3CN)_4^+$ through solvent loss, with the resultant "$Cu_4Bi_2I_{10}$" composition being unstable with respect to the simple binary iodides. However, the release of CH_3CN in **1** results in a "$(n\text{-}Bu_4N)_2(Cu_2Bi_2I_{10})$" composition, which is still a thermally stable phase.

Conclusion

We have synthesized a series of heterometallic copper iodobismuthates with a tetranuclear $[Cu_2Bi_2I_{10}]^{2-}$ building unit as 0-D tetranuclear anion clusters (**1**), 1-D linear anionic polymers (**2**), and 1-D ladderlike anionic chains (**3**) by utilizing different cations. Their optical properties reveal a structure-related band-gap decrease that is further supported by the DFT calculations. The essential evolvements of the optical absorption spectra between corresponding M/Bi/I (M = Bi, Cu, or Ag) compounds are compared. Interestingly, compounds **1**−**3** show very different thermal stabilities: **2** is the most stable; **1** undergoes a solvent release at 85 °C to form a **1-A** phase that melts congruently at 145 °C and finally decomposes at 230 °C; **3** releases CH_3CN at 80 °C and decomposes primarily into BiI_3 and CuI. In M/Bi/I systems (M = Cu or Ag), we have so far found variations in both the structures and the properties and have uncovered some essential differences in their electronic structures. More explorations are ongoing on other heterometallic M/Bi/I systems aimed at the possible formation of novel structures and a deeper understanding of their structure−property relationships.

Acknowledgment. This research was supported by the National Natural Science Foundation of China (Projects 20401014, 20401013, and 20521101), the State Key Laboratory Science Foundation (Projects 070023 and 050097), the NSF of Fujian Province (Projects 2004HZ01-1, 2005HZ01-1, and 2006J0271), and the "Key Project from CAS" (Project KJCX2-YW-H01).

Supporting Information Available: X-ray data in the form of a CIF file for compounds **1**−**3**, supporting figures, and the details of crystallographic data. This material is available free of charge via the Internet at http://pubs.acs.org.

IC700904D